Pergamon

Cement and Concrete Research 33 (2003) 1–7

CEMENT AND CONCRETE RESEARCH

Study of chloride binding and diffusion in GGBS concrete

Rui Luo[a,*], Yuebo Cai[b], Changyi Wang[b], Xiaoming Huang[a]

[a]*Transportation College of Southeast University, Nanjing 210096, China*
[b]*Nanjing Hydraulic Research Institute, Nanjing 210029, China*

Received 1 August 2001; accepted 10 December 2001

Abstract

Ordinary Portland cement (OPC) and OPC/ground granulated blastfurnace slag (GGBS) 70%, with or without 5% sulfates, were widely investigated in respect to their pore structures, chloride diffusion coefficients, internal and external chloride-binding capabilities by expression method and leaching method and the microstructure analysis on Friedel's salt such as differential thermal analysis (DTA), X-ray diffraction (XRD) and scanning electron microscopy (SEM). It can be concluded that GGBS can improve the pore structure of OPC and decrease the chloride diffusion coefficient greatly, and that sulfates do not do good for the pore structure and chloride diffusion for GGBS. GGBS increases the chloride-binding capability greatly without reference to the internal or external chloride and sulfates decrease the chloride-binding capability of GGBS greatly. It can be also found that the maximum intensity peak corresponding to Friedel's salt appears at about 8.0 Å, its endothermic effect appears at about 360 °C, its morphology is hexagonal slice whose size is about 2–3 μm; that the output of Friedel's salt formed by GGBS is much more than OPC; and that sulfates influence the output of Friedel's salt greatly. The corresponding mechanism was also analyzed.

Keywords: Ground granulated blastfurnace slag (GGBS); Chloride binding; Diffusion; Sulfate; Friedel's salt

1. Introduction

Chloride-induced corrosion of reinforcing steel in concrete structures has become a widespread durability problem throughout the world and many researchers [1–10] have researched about it. It has been proved that ground granulated blastfurnace slag (GGBS) has perfect performance to resist chloride-induced corrosion, especially chloride-binding capability [5,9,11]; however, most researches were about internal chloride-binding capability that is not appropriate to the practice completely, so the external chloride-binding capability of GGBS needs to be researched clearly. In China, the output of slag is very large and the slag has to be reused efficiently, so it is necessary to have a detailed research about it.

In China, the output of gypsum is also large and it is also necessary to reuse the gypsum efficiently, so some researches intended to reuse the GGBS blended with some gypsum because sulfates may improve the pore structure and decrease the chloride diffusion coefficient for the expanding reaction between sulfates and C_3A, though sulfates may influence the chloride-binding capability for GGBS [9,10]. Thus, details about the effects of sulfates on the performance of GGBS to resist chloride-induced corrosion should also be known clearly.

It is well known that chloride-binding capability is related to the formation of Friedel's salt, but the research about Friedel's salt is still few, especially its morphology.

The performance of GGBS was widely researched in this study with regard to its pore structure, chloride diffusion coefficient, chloride-binding capability and the microstructure analysis on Friedel's salt by differential thermal analysis (DTA), X-ray diffraction (XRD) and scanning electron microscopy (SEM).

2. Experimental details

2.1. Materials

The composition of the cement clinker and GGBS used in the experimentation was given in Table 1. The specific area of GGBS was 4650 cm^2/g. Sulfates such as $CaSO_4$ and Na_2SO_4 were used.

* Corresponding author. Tel.: +86-25-579-1654; fax: +86-25-579-1654.
E-mail address: Luoruiseu@sohu.com (R. Luo).

0008-8846/03/$ – see front matter © 2003 Elsevier Science Ltd. All rights reserved.
PII: S0008-8846(02)00712-3

Table 1
Chemical analysis of OPC and GGBS(%)

	SiO_2	Al_2O_3	Fe_2O_3	CaO	MgO	f-CaO	K_2O	SO_3
OPC	21.87	4.91	5.40	66.02	0.94	0.93	0.916	2.23
GGBS	31.75	13.84	3.79	40.40	8.2			0

2.2. Experiment for pore structure and chloride diffusion coefficient of concrete

The mortar specimens which were gotten by sieving the just mixed concretes were used to measure the pore structure of concrete, and the pore structure of the mortar can be measured by mercury pressure. The cure times for mortars were 28 and 60 days. The specimens of concrete to measure the chloride diffusion coefficients were cured at the standard state for 28 days, then they were immersed in marine water with five sides of each specimen covered with epoxy, and 6 months later, the powder at five different depth layers was collected with a drill. The five different depths were 0–10, 10–20, 20–30, 30–40 and 40–50 mm from the chloride diffusion surface of the specimen. Both the total diffused chloride content and the free chloride content were measured for the total chloride diffusion coefficient and the free chloride diffusion coefficient of concrete. Ten grams of dry powder of each layer was completely dissolved with 100 ml of HNO_3 solution diluted with 6 N HNO_3 and distilled water (volume ratio was 15:85), then the dissolved solution was filtrated. A certain amount of the filtrated solution was taken out, enough 0.02 N $AgNO_3$ solution was added, three to five drops of iron alum solution added, then titrated with 0.02 N KCNS solution until the solution become red and the red color can be maintained for 5–10 s, so the total chloride ion content can be obtained. Another 10 g of dry powder was dissolved with 200 ml of distilled water, then the dissolved solution was titrated with 0.02 N $AgNO_3$ solution and phenolphthalein was used as an indicator, so the free chloride content can also be obtained. The total chloride diffusion coefficients and the free chloride diffusion coefficients can be calculated according to the chloride content at different depths of concrete. The mixed ratio (water: binder:sand:aggregate) for the three kinds of concretes was 0.34:1:1.7:3.29. The binder of GGBS concrete is 30% ordinary Portland cement (OPC) and 70% GGBS and that of GGBS concrete with some gypsum is 30% OPC, 65% GGBS and 5% gypsum.

2.3. Experiment for expression method

Pastes and mortars, whose mixed ratios were shown in Table 3, were used to analyze the internal chloride-binding capability. Sodium chloride (1.0% by weight of binder) was introduced at the time of mixing. Both the mortars and the pastes were cast in $\varphi 5 \times 7.5$ cm cylindrical impermeable plastic molds, sealed and stored at 20 ± 2 °C. After 1 1/2 months of curing in sealed containers, triplicate specimens were demolded and immediately placed in a cylindrical pore solution expression device similar to that described by Diamond [6]. Pressure was gradually increased to between 350 and 510 MPa, and the pore fluid was collected with an injector. The collected pore fluid was diluted by 100 ml of deionized water, chloride concentration of the diluted fluid was determined by titration with $AgNO_3$ solution, and

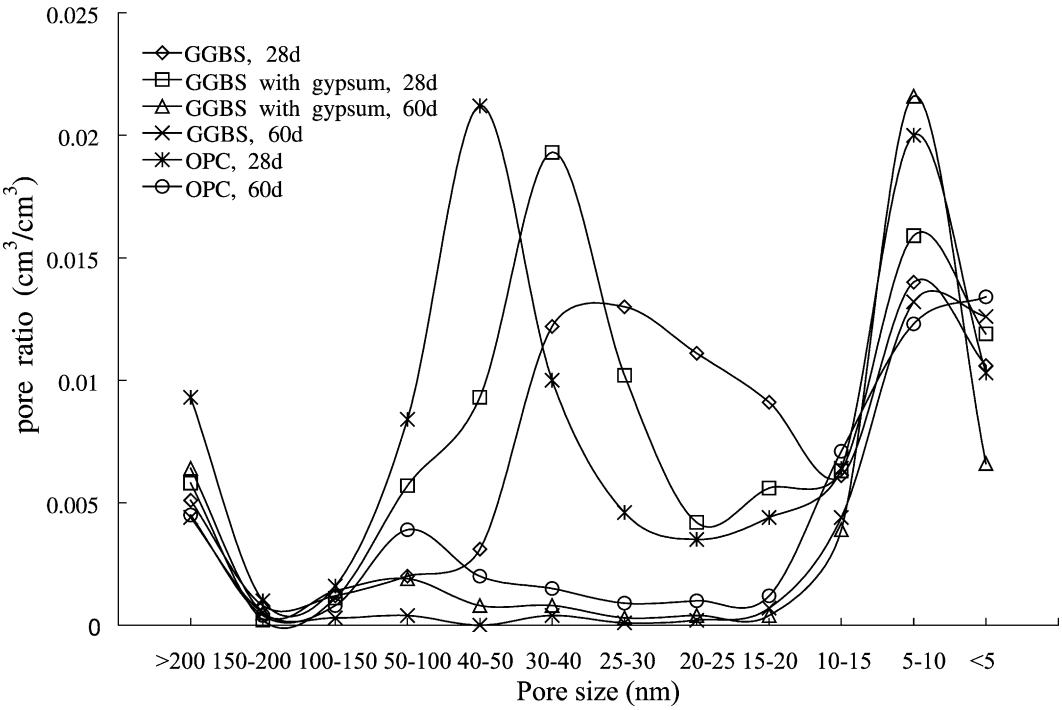

Fig. 1. Pore structure for the three concretes.

Table 2
Chloride diffusion coefficient of concrete (10^{-8} cm^2/s)

	OPC concrete	GGBS concrete	Concrete with gypsum
Total chloride	3.02	1.95	2.44
Free chloride	2.65	1.58	2.14

OH^- concentration was determined by titration with 0.01 N HCl solution using phenolphthalein as indicator.

Evaporable water on parallel specimens was determined on parallel specimens at 105 ± 5 °C, based upon which the bound chloride was determined. Xu [9] heated the parallel specimens above 1000 °C to get the nonevaporable water content to estimate the bound chloride content, but the carbonate will be decomposed at that high temperature and the nonevaporable water obtained will be not correct, so the effect of hydration was corrected only by the evaporable water in this research.

2.4. Experiment for leaching method

The external chloride-binding performance of GGBS was researched by the leaching method. The mixed ratio of pastes and mortars was shown in Table 4. All the specimens were cured at 20 ± 2 °C. The samples were made according to Tang and Nilsson [7]. The content of bound chlorides was calculated by the following equations (Eqs. (1)–(4)):

$$C_{b1} = \frac{35.45V(c_0 - c_1)}{W_{gel}} \quad (1)$$

$$W_{gel} = \frac{(1 + W_n^0 f_c \alpha)}{1 + W_n^0 f_c \alpha} W \quad (2)$$

$$f_c = \frac{W_{cement}}{W_{cement} + W_{aggregates}} \quad (3)$$

$$C_{b2} = \frac{34.45[c_0 V - c_1 V' - c_2(V + V'' - V')]}{W_{gel}} \quad (4)$$

where C_{b1} and C_{b2} are total bound chloride content and chemical-bound chloride content, mg/g; V, V' and V'' are volume of solution, volume of solution removed including first titration and volume of deionized water added, ml; c_0, c_1 are initial concentration and equilibrium concentration of chloride solution, mol/l; W, W_{gel} are weight of dry sample and weight of the gel, g; W_n^0 is nonevaporable water, assuming $W_n^0 = 0.25$; f_c is cement content in concrete by weight; and α is degree of hydration, which was measured by the parallel specimen according to the following equation: $\alpha = W_1/W_n^0$, where W_1 is the content of unhydrated water in the parallel specimen measured at 105 ± 5 °C.

3. Results

3.1. Pore structure and chloride diffusion coefficients of concrete

The pore structure of the mortars was shown in Fig. 1. It can be clearly seen that the coarse pores of GGBS concrete were much less and the pore structure of OPC concrete was improved greatly when 70% GGBS was added, especially for the pore structure for the time of 60 days. But sulfates did not improve the pore structure of GGBS as expected, and it surely shows that some other causes, except the expanding reaction between sulfates and C_3A, influence the pore structure of concretes. Thus, it is not right to improve the pore structure of GGBS concrete with sulfates.

The chloride diffusion coefficients of the three kinds of concretes were measured for further research. Both the total chloride diffusion coefficient and the free chloride diffusion coefficient were determined, as shown in Table 2. The total chloride diffusion coefficient is the coefficient for all the diffused chlorides including the bound chloride by the concrete and the free chloride diffusion coefficient is only for the unbound chloride diffused to the concrete. Table 2 shows that both the total chloride diffusion coefficient and the free chloride diffusion coefficient decreased greatly when 70% GGBS was added; thus, it can be concluded that GGBS is good in decreasing the chloride diffusion coefficient. But the chloride diffusion coefficient increased greatly when 5% gypsum was added. So it is not right to

Table 3
Internal chloride-binding capability for mortars and pastes

Code	Mixed ratio (B:W:S)	Binder and content (%)	OH^- (mg/g)	Cl_{total}^- (mg/g)	Cl_{free}^- (mg/g)	Cl_{bound}^- (mg/g)
M1	1:0.6:3	C(100)	2.492	6.065	1.186	4.879
M2	1:0.6:3	C(30) + G(70)	2.224		0.519	5.546
M3	1:0.6:3	C(30) + G(65) + CS(5)	1.939		1.512	4.553
M4	1:0.6:3	C(30) + G(65) + NS	6.550		3.107	2.958
P1	1:0.4	C(100)	2.270	6.065	1.336	4.729
P2	1:0.4	C(30) + G(70)	1.918		0.519	5.546
P3	1:0.4	C(30) + G(65) + CS(5)	1.582		1.706	4.359
P4	1:0.4	C(30) + G(65) + NS	4.153		3.621	2.444

M1, M2, M3 and M4 denote OPC mortars, GGBS mortar, GGBS mortar with 5% $CaSO_4$ and GGBS mortar with Na_2SO_4. P1, P2, P3 and P4 denote OPC pastes, GGBS paste, GGBS paste with 5% $CaSO_4$ and GGBS paste with Na_2SO_4. OH^- denotes the collected OH^- content of the expression pore solution. Cl_{total}^- denotes the total chloride added; Cl_{free}^- and Cl_{bound}^- denote the unbound chloride and the bound chloride.

Table 4
Unit gel's bound chloride content for mortar

Code	Mixed ratio (B:W:S)	Binder and content (%)	C_{b1} (mg/g)	C_{b2} (mg/g)	C_{b3} (mg/g)
P11	1:0.4	C(100)	2.627	1.618	1.009
P12	1:0.4	C(30)+G(70)	3.758	2.921	0.837
P13	1:0.4	C(30)+G(65)+CS(5)	2.787	2.013	0.774
P14	1:0.4	C(30)+G(65)+NS	1.156	0.587	0.569
M11	1:0.6:3	C(100)	3.344	1.097	2.253
M12	1:0.6:3	C(30)+G(70)	7.270	3.732	3.538
M13	1:0.6:3	C(30)+G(65)+CS(5)	5.331	1.916	3.415
M14	1:0.6:3	C(30)+G(65)+NS	2.784	1.024	1.760

P11, P12, P13 and P14 denote OPC pastes, GGBS paste, GGBS paste with 5% $CaSO_4$ and GGBS paste with Na_2SO_4. M11, M21, M31 and M41 denote OPC mortars, GGBS mortars, GGBS mortars with 5% $CaSO_4$ and GGBS mortars with Na_2SO_4 whose SO_4^{2-} content is the same as that from $CaSO_4$, C, G, CS and NS denote OPC, GGBS, $CaSO_4$ and Na_2SO_4, and C_{b1}, C_{b2} and C_{b3} denote the total chloride-binding content, chemical-binding content and physical chloride-binding content. B, W and S denote binder, water and sand.

decrease the chloride diffusion coefficient for the expanding reaction caused by sulfates in our tests. It can be also seen that the free chloride diffusion coefficient was smaller than the total chloride diffusion coefficient because some chloride ions were bound. The free chloride diffusion coefficient of GGBS concrete drops more than the others, and this result can be explained by the fact that the bound chloride ions by GGBS concrete were more than those by the others.

3.2. Internal chloride-binding capability

Table 3 shows that the internal chloride-binding capability of pastes and mortars increases greatly when 70% OPC is substituted by GGBS, and it also shows clearly that sulfates drop the internal chloride-binding capability greatly and the alkalinity of sulfates also influences the chloride-binding capability greatly, e.g., the higher the alkalinity of sulfate, the lower is the chloride-binding capability.

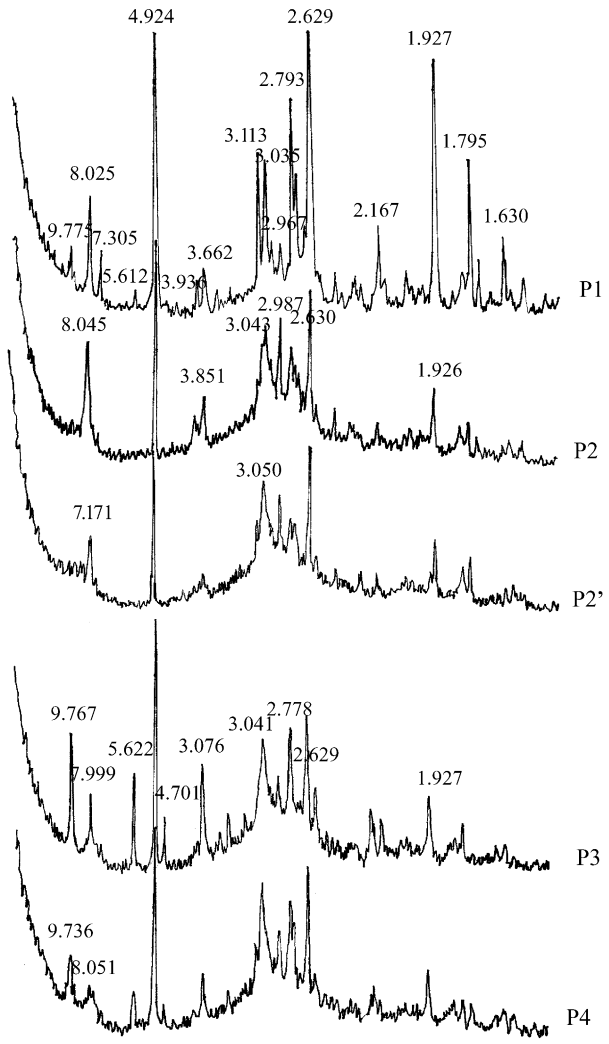

Fig. 2. X-ray diffractograms for pastes.

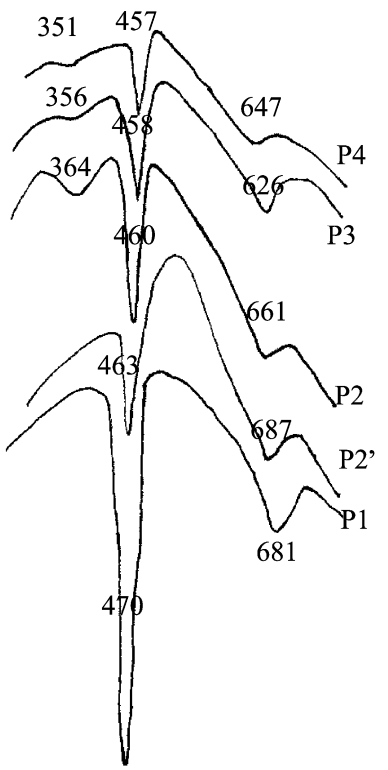

Fig. 3. DTA thermograms for Friedel's salt and $Ca(OH)_2$.

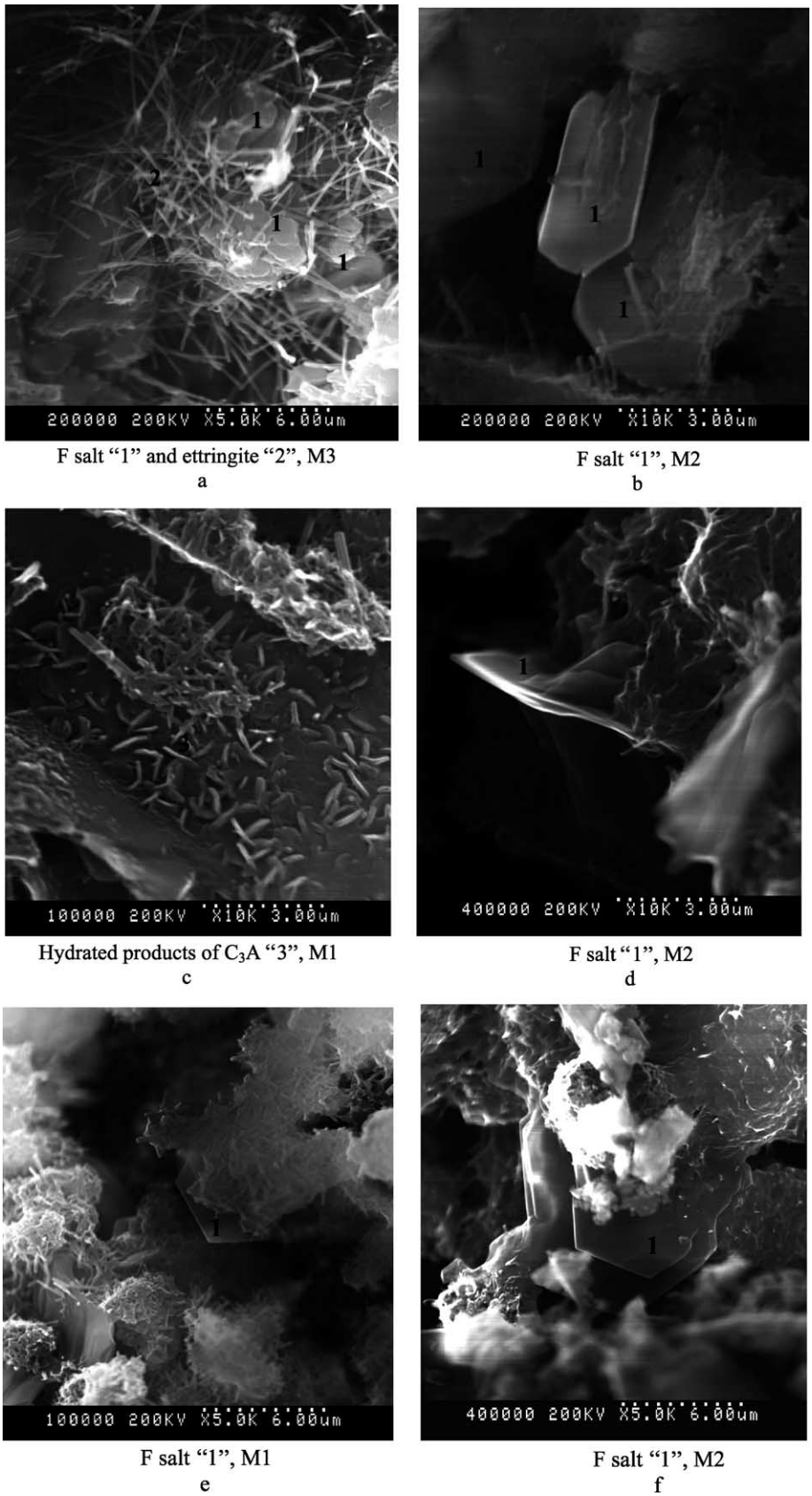

Fig. 4. Photos for Friedel's salt and ettringite, the hydrated products of C_3A.

3.3. External chloride-binding capability

Table 4 lists the external chloride-binding capability of mortars, including physical binding content and chemical binding content. For convenience, all the values given in the table were denoted as the content of the unit binder. All the mortars were cured for 28 days and the hydration coefficient of mortar was determined with the parallel specimens.

The external chloride-binding capability (shown in Table 4) also indicates that GGBS benefits from the chloride binding, and that sulfates and their alkalinity do harm to chloride binding. It can also be seen that it is mainly the chemical chloride-binding capability that improves the chloride-binding capability of GGBS greatly.

3.4. DTA, XRD and SEM results

The pastes for DTA and XRD tests were the same with the specimens for the expression method, and P1, P2, P3, P4 and P2′ in Figs. 2 and 3, respectively, denoted OPC paste, GGBS paste, GGBS paste with 5% $CaSO_4$, GGBS paste with Na_2SO_4 and GGBS paste without any chloride added. The mortars used for the SEM test were mortars similar to the specimens for the expression method.

Fig. 2 shows the X-ray diffractograms for hydrated pastes. It can be clearly seen that the maximum intensity peak corresponding to the Friedel's salt appears at about 8.0 Å and the GGBS paste without any chloride does not show this kind of peak at the corresponding position. The intensity of the maximum peak of the Friedel's salt is much lower than that of GGBS paste when some sulfates were added. Moreover, the intensity of P4 added with Na_2SO_4 is still lower than that with $CaSO_4$. Both P3 and P4 formed the ettringite at about 9.7 Å, but it cannot be seen clearly in P2 for the formed ettringite is much less. The corresponding peaks for $Ca(OH)_2$ are at about 4.9, 2.6, 1.9 and 1.795 Å. We can also see that the corresponding peak intensity of Friedel's salt for P1 is high, too. Does it mean that OPC paste can also form lots of Friedel's salt?

Unfortunately, C_4AH_{13}, a hydrate of C_3A, also has the maximum intensity peak at about this position, and this makes the identification of Friedel's salt more complicated. So DTA was used to make a distinction between Friedel's s salt and C_4AH_{13}, and the DTA results were shown in Fig. 3. It can be seen that Friedel's salt yields an endothermal effect at around 360 °C, and it can be seen clearly that the endothermal peak area of Friedel's salt for P2 is much larger than that added with some sulfates. Moreover, the higher the alkalinity of sulfate, the smaller is the peak area. But no clear endothermal peak appears at the corresponding position for the GGBS paste without any chloride added, and neither does the OPC paste appear. This can identify that the maximum intensity peak at about 8.0 Å in P2 is mainly for Friedel's, but that in P1 is mainly for C_4AH_{13} and not for Friedel's salt.

Fig. 4 clearly shows the morphology of Friedel's salt, ettringite and the hydrated product of C_3A. It can be easily seen that the morphology of Friedel's salt is hexagonal slice and its size is between 2 and 3 μm. The hydrated products of C_3A are also hexagonal, but its size is no more than 1 μm and is much smaller than that of Friedel's salt. Although the photo in Fig. 4b may be $Ca(OH)_2$, since the photo for $Ca(OH)_2$ may also be hexagonal, we also think it more reasonable that it is the photo for Friedel's salt because the ordinary size of $Ca(OH)_2$ is much larger. The fact that it is difficult to find Friedel's salt in M1 and it is easy to find it in M2 tells that GGBS paste formed much more than Friedel's salt. The fact that it is difficult to find ettringite in M2 and it is easy to find it in GGBS pastes, with some sulfates added and with the coexisting phenomenon of F salt and ettringite in M3 mortars, indicates that competition exists between chloride ions and sulfate ions.

4. Discussion

In our tests, sulfates neither improve the pore structure of GGBS obviously, nor decrease the chloride diffusion coefficient, so it definitely some other factors, such as the chloride-binding capability, except the expanding reaction between sulfates and C_3A, that influence the chloride diffusion coefficient. So it is not right to decrease the chloride diffusion coefficient with some sulfates added.

Regardless of internal or external chloride, GGBS can greatly increase the chloride-binding capability, especially the chemical chloride-binding capability, but sulfates decrease the chloride-binding capability of GGBS greatly. It is well known that C_3A can form an insoluble complex, calcium chloroaluminate hydrate (Friedel's salt) [13], with chloride ions in hydrated cement pastes. So the reason as to why GGBS can increase the chloride-binding capability can be explained easily, e.g., GGBS can form more Friedel's salt. This can be verified from the microstructure analysis above. The microstructure analysis shows that GGBS can form more Friedel's salt, so GGBS can bind more chloride ions. Why sulfates influence the chloride-binding capability is because of the preferential reaction between sulfates and C_3A. More C_3A reacts with sulfates; less C_3A can bind the chloride to form Friedel's salt. This can also be verified by the XRD and DTA results. The XRD and DTA results indicate that no distinct ettringite exists in GGBS paste with or without chloride, but the peak for the ettringite is distinct and the intensity of the Friedel's salt is much lower for sulfate pastes because of the added sulfate. The DTA results also indicate that the peak area of Friedel's salt decreases greatly when some sulfates are added. Moreover, the coexisting phenomenon of Friedel's salt and ettringite in photos shown in Fig. 4a, in which Friedel's salt exists among ettringite, can clearly prove that the competition exists between sulfate ions and chloride ions. So, sulfate decreases the chloride-binding capability greatly. Obviously, the lower content of sulfate of GGBS is one of the reasons that GGBS has perfect performance to resist the chloride-induced cor-

rosion because the effect of sulfate on the chloride binding is less.

According to Ref. [12], the structure of C_4AH_{13} and its homogeneous hydrate, e.g., the hydrated products of C_3A, can be denoted as $2[Ca_2Al(OH)_6{\cdot}OH{\cdot}H_2O]$. The OH^- ion is very weak and can be exchanged for some other negative ions, such as chloride ion, because the OH^- ion is attracted by the electrovalent bond to form Friedel's salt. Of course, alkalinity can influence this kind of exchange to bind the chloride to the released OH^- ion during the exchange progress. So the higher the alkalinity of the sulfate, the lower is the chloride-binding capability.

5. Conclusions

(1) GGBS can improve the pore structure of OPC concrete and decrease the chloride diffusion coefficient greatly. Sulfates cannot improve the pore structure of GGBS concrete and decrease the chloride diffusion coefficient of GGBS concrete.

(2) Regardless of internal or external chloride, GGBS can increase the chloride-binding capability greatly, especially the chemical chloride-binding capability, but sulfates and alkalinity decrease the chloride-binding capability greatly.

(3) Friedel's salt appears at about 8.0 Å, its endothermal peak is at about 360 °C and its morphology is hexagonal slice whose size is between 2 and 3 μm.

(4) The fact that GGBS can form more Friedel's salt is the reason why GGBS can increase the chloride-binding capability, and the reason why sulfate and alkalinity influence the chloride binding is the competition among sulfate ions, hydroxyl ions and chloride ions during the formation of Fridel's salt.

References

[1] C. Arya, J.B. Newmen, An assessment of four methods of determining the free chloride, Mater. Struct. 23 (1990) 319–330.
[2] B.B. Hope, J.A. Page, J.S. Poland, The determination of the chloride content of concrete, Cem. Concr. Res. 15 (1985) 863–870.
[3] A.K. Suryavanshi, J.D. Scantlebury, S.B. Lyon, Mechanism of Friedel's salt formation in cements rich in tri-calcium aluminate, Cem. Concr. Res. 26 (1996) 717–727.
[4] M.N. Haque, O.A. Kayyali, Aspects of chloride ion determination in concrete, ACI 92 (1995) 532–540.
[5] R.K. Dhir, M.A.K. El-Mohr, T.D. Dyer, Chloride binding in GGBS concrete, Cem. Concr. Res. 26 (1996) 1767–1773.
[6] S. Diamond, Chloride concentrations in concrete pore solutions resulting from calcium and sodium chloride admixtures, Cem., Concr. Aggregates 8 (1986) 97–102.
[7] L. Tang, L. Nilsson, Chloride binding capacity and binding isotherms of OPC pastes and mortars, Cem. Concr. Res. 23 (1993) 247–253.
[8] R.S. Barneyback, Expression and analysis of pore fluids from hardened cements and mortars, Cem. Concr. Res. 11 (1981) 271–285.
[9] Y. Xu, The influence of sulfates on chloride binding and pore solution chemistry, Cem. Concr. Res. 27 (1997) 1841–1850.
[10] S. Ehtesham Hussain, Rasheeduzzafar, Influence of sulfates on chloride binding in cements, Cem. Concr. Res. 24 (1994) 8–24.
[11] D.M. Roy, G.M. Idorn, Hydration, structure, and properties of blast furnace slag cements, mortars and concrete, ACI 26 (1992) 43–79.
[12] C.L. Page, N.R. Short, A.E. Tarras, Diffusion of chloride ions in hardened cement pastes, Cem. Concr. Res. 11 (1981) 395–406.
[13] F.M. Li, The Chemistry of Cement Concrete, China Construction Industry Publishing House, Beijing, 1980, pp. 256–290 (M. Tang, Trans.).